

Effects of substrate misorientation and growth rate on ordering in GaInP

L. C. Su, I. H. Ho, and G. B. Stringfellow

Departments of Materials Science and Engineering and Electrical Engineering, University of Utah, Salt Lake City, Utah 84112

(Received 22 October 1993; accepted for publication 20 January 1994)

Epitaxial layers of $\text{Ga}_x\text{In}_{1-x}\text{P}$ with $x \approx 0.52$ have been grown by organometallic vapor-phase epitaxy on GaAs substrates misoriented from the (001) plane in the $[\bar{1}10]$ direction by angles ϑ_m , of 0° , 3° , 6° , and 9° . For each substrate orientation growth rates r_g of 1, 2, and $4 \mu\text{m/h}$ have been used. The ordering was characterized using transmission electron diffraction (TED), dark-field imaging, and photoluminescence. The (110) cross-sectional images show domains of the Cu-Pt structure separated by antiphase boundaries (APBs). The domain size and shape and the degree of order are found to be strongly affected by both the substrate misorientation and the growth rate. For example, lateral domain dimensions range from 50 \AA for layers grown with $r_g = 4 \mu\text{m/h}$ and $\vartheta_m = 0^\circ$ to 2500 \AA for $r_g = 1 \mu\text{m/h}$ and $\vartheta_m = 9^\circ$. The APBs generally propagate from the substrate/epilayer interface to the top surface at an angle to the (001) plane that increases dramatically as the angle of misorientation increases. The angle is nearly independent of growth rate. From the superspot intensities in the TED patterns, the degree of order appears to be a maximum for $\vartheta_m \approx 5^\circ$. Judging from the reduction in photoluminescence peak energy caused by ordering, the maximum degree of order appears to occur at $\vartheta_m \approx 4^\circ$.

I. INTRODUCTION

Atomic-scale ordering is a naturally occurring phenomenon widely observed in III/V alloys.¹ This phenomenon involves the formation of monolayer superlattice structures along a particular crystallographic direction in the lattice. For (001)-oriented substrates, the Cu-Pt ($L1_1$) structure, with ordering on {111} planes, is most commonly observed. Only two variants of the Cu-Pt structure are produced during growth on (001)-oriented substrates, i.e., of the four equivalent {111} planes, ordering occurs on only two, ($\bar{1}11$) and ($1\bar{1}1$). Misorientation of the (001) substrate by a few degrees in the $[\bar{1}10]$ direction, to give $[\bar{1}10]$ -oriented steps on the surface, is found to result in the formation of only one variant. Growth on grooved substrates shows that steps moving in opposite directions are responsible for formation of the two variants observed.^{1,2} These observations have led to the development of several kinetic models to explain the ordering phenomena,¹⁻⁴ including a model based on the differential attachment of adatoms at $[\bar{1}10]$ steps that interact with $[\bar{1}10]$ dimer rows on the (2×4) reconstructed (001) surface.^{1,2} As would be expected for a kinetically controlled process, increasing the growth rate generally decreases the degree of order. Cao *et al.*⁵ demonstrated that high growth rates of $12 \mu\text{m/h}$ yield nearly completely disordered GaInP. The effects of these and other growth parameters on ordering, determined from the band gap measured using photoluminescence spectroscopy, have recently been studied systematically by Kurtz *et al.*⁶ They astutely point out that the surface kinetic limitation, described above, is important only in a certain range of growth parameter space, most important at relatively low growth temperatures. At growth temperatures of, for example, 700°C the degree of order decreases and, at these temperatures, low growth rates ($< 2 \mu\text{m/h}$) also give less ordering. This is attributed to "annealing" effects during growth whereby the structure below the surface reverts to the

thermodynamically stable disordered state during the time the sample is held at a relatively high temperature during growth.

The degree of order and the ordered structure formed during growth also depend strongly on the substrate orientation.^{1,6-8} As mentioned, growth on (001)-oriented substrates generally produces material with the Cu-Pt structure, while growth on (110) substrates produces material with the Cu-Au structure, with ordering on {100} planes.^{9,10} Little, if any, ordering is observed for growth on (111),^{11,12} (221),¹³ (311),¹³ and (511) (Ref. 14) -oriented substrates. In fact, growth on faceted surfaces with adjacent (001)- and $(\bar{1}\bar{1}5)$ -oriented areas yields adjacent regions of highly ordered and disordered material.¹⁵ This has allowed the direct demonstration that Cu-Pt ordering leads to a reduction in energy band gap of $> 100 \text{ meV}$ for $\text{Ga}_{0.52}\text{In}_{0.48}\text{P}$ alloys,¹⁵ as anticipated from the calculations of Wei and Zunger.¹⁶ Thus, ordering is of significant practical importance. It must be avoided in short-wavelength lasers and light-emitting diodes.¹¹ On the other hand, a reduction of band gap may be beneficial for InAsSb alloys for infrared detectors operating in the $8\text{--}12 \mu\text{m}$ wavelength regime.¹⁷

This article presents the results of a systematic study of the effects of both growth rate and the angle of substrate misorientation on ordering, in particular the domain size and shape and the degree of order. A matrix of growth rates from 1 to $4 \mu\text{m/h}$ and substrate misorientations of 0° , 3° , 6° , and 9° was explored.

II. EXPERIMENT

The GaInP epitaxial layers were grown by organometallic vapor-phase epitaxy (OMVPE) on semi-insulating GaAs substrates misoriented by 0° , 3° , 6° , and 9° ($\pm 0.5^\circ$) in the $[\bar{1}10]$ direction, to produce various densities of $[\bar{1}10]$ -oriented steps on the surface. Substrate preparation consisted of degreasing in trichloroethane, acetone, and methanol fol-

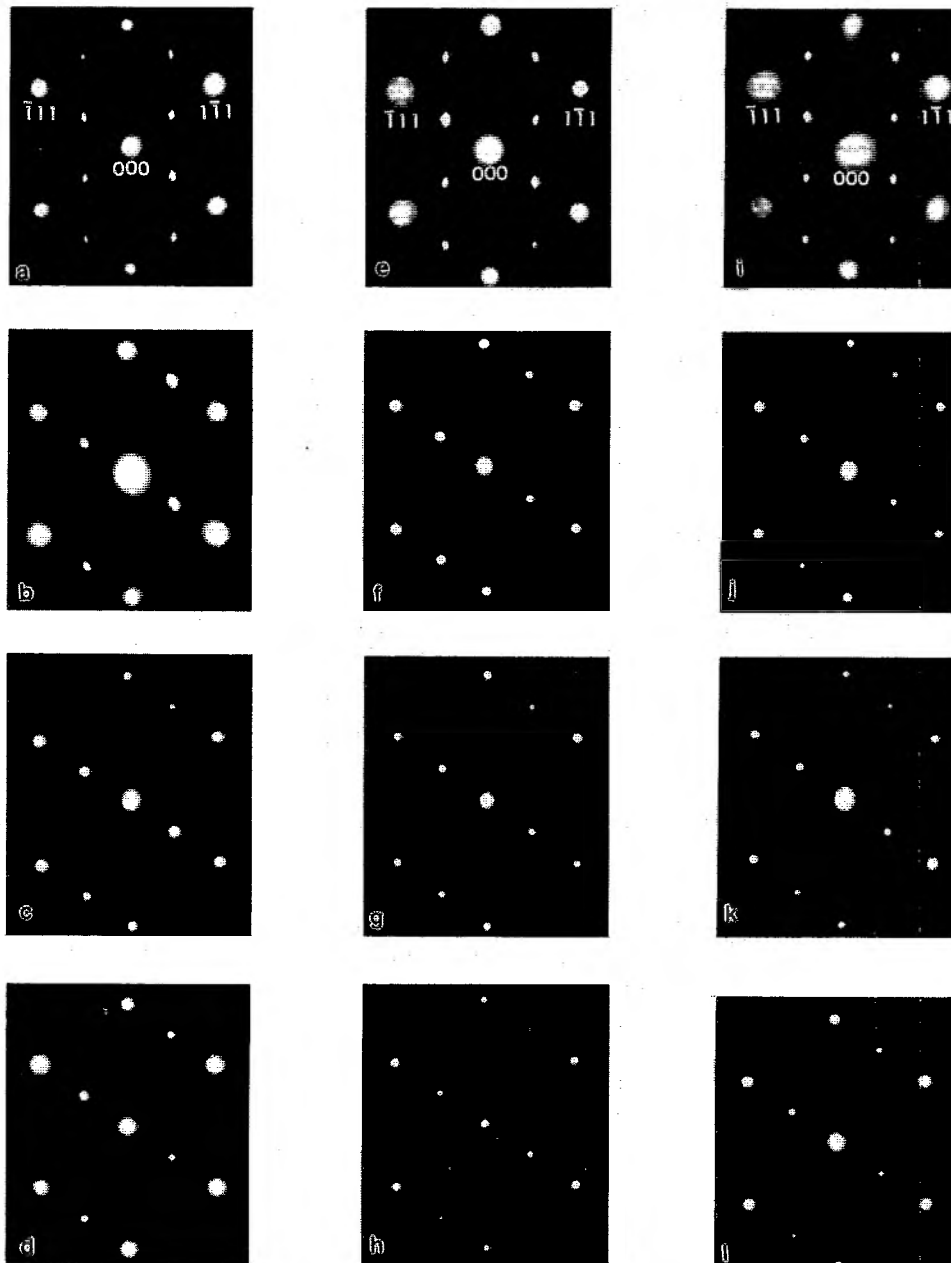


FIG. 1. [110] transmission electron-diffraction patterns obtained for samples of GaInP grown with various growth rates and substrate misorientations. The patterns are arranged in a matrix reflecting the growth conditions. The columns represent growth rates of 4 (a,b,c,d), 2 (e,f,g,h), and 1 (i,j,k,l) $\mu\text{m/h}$. The rows represent the values of ϑ_m : 0° (a,e,i), 3° (b,f,j), 6° (c,g,k), and 9° (d,h,l).

lowed by a 5 min etch in a 1% bromine in methanol solution. The substrates were then rinsed in methanol and blown dry with N_2 , after which they were immediately loaded into the quartz reactor tube. A horizontal, atmospheric pressure OMVPE reactor was used. The source materials were trimethylgallium (TMGa at -9°C), trimethylindium (TMIn at 25°C), and phosphine. The carrier gas was Pd-diffused hydrogen with a flow rate of 4 slm. The growth temperature and V/III ratio were constant at 670°C and 160, respectively. The growth rate was varied by changing the input molar flow rate of the TMGa and TMIn, keeping the input V/III ratio constant. The GaInP layers were typically approximately 1

μm thick. Before beginning the GaInP growth, a $0.15\ \mu\text{m}$ GaAs buffer layer was first deposited using TMGa and arsine at a temperature and V/III ratio of 670°C and 80, respectively, to improve the quality of the GaInP layers.

The surface morphologies and thicknesses of the GaInP epilayers were observed using a Nomarski differential interference contrast optical microscope. The solid composition of the GaInP layers was measured by x-ray diffraction, using a Diano XRD 8000 diffractometer with Cu radiation. The position of the (004) peak for the epilayer relative to that of the GaAs substrate was used to determine the lattice constant and, using Vegard's law, the solid composition. For misori-

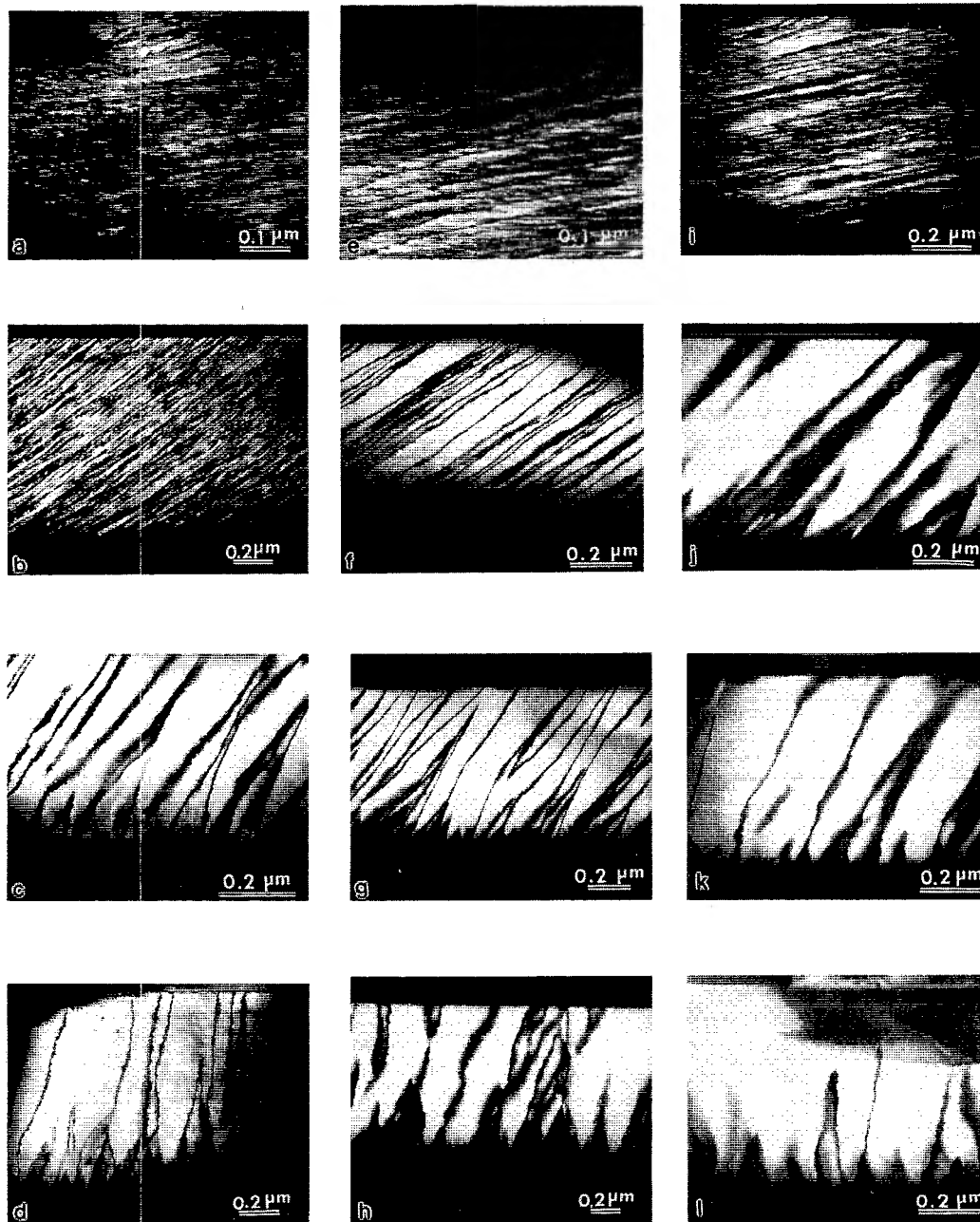


FIG. 2. Dark-field transmission electron microscope images, obtained using the $\frac{1}{2}(1\bar{1}3)$ diffraction spot, of the GaInP samples arranged in the same matrix as for Fig. 1, i.e., the first, second, and third columns represent growth rates of 4, 2, and 1 $\mu\text{m/h}$ and the four rows represent, from top to bottom, substrate misorientations of 0°, 3°, 6°, and 9°.

ented substrates, a simple goniometer was used to properly orient the substrate.

The cross-section transmission electron microscope (TEM) samples were prepared by mechanically thinning and polishing samples glued face to face to a thickness of approximately 10 μm , followed by Ar-ion milling at 77 K. The $[110]$ and $[\bar{1}10]$ directions in the GaAs substrates were determined from etch pit anisotropy characteristics. The transmission electron diffraction (TED) patterns and TEM images were obtained at an incident electron energy of 200 kV using a JEOL 200CX scanning transmission electron microscope.

A two-beam technique was used to obtain the dark-field images.

The 10 K photoluminescence (PL) spectra were excited with the 488 nm line of an Ar^+ laser. The emission was dispersed using a Spex Model 1870 monochromator and detected using a Hamamatsu R1104 head-on photomultiplier tube.

III. RESULTS

The surface morphologies of every epitaxial layer described in this section were mirrorlike to the naked eye and

virtually featureless when viewed by interference contrast optical microscopy. The lack of observable cross-hatch pattern and the results of the x-ray-diffraction measurements both indicate that the values of x for these alloys are 0.52 ± 0.01 for most of the layers. The specific values of x measured by x-ray diffraction, assuming that any lattice mismatch is accommodated elastically, for the various samples studied are given in Table I.

TED patterns for the matrix of layers grown with various growth rates and substrate misorientations are shown in Fig. 1. It should be noted that a comparison of absolute intensities of the superlattice spots is nearly meaningless because of the different sample thicknesses and photographic exposure times used. The relative degree of order can, for some samples, be judged by observing the intensity of the $\frac{1}{2}\{111\}$ superlattice spot relative to that of the corresponding $\{111\}$ zinc-blende lattice spot, as is discussed below.

Considering first the layers with $\vartheta_m = 0^\circ$, the TED patterns for all growth rates have superlattice spots at $\frac{1}{2}(\bar{1}11)$ and $\frac{1}{2}(1\bar{1}1)$, indicating the presence of two variants of the Cu-Pt structure. This is consistent with previous observations by several groups.^{1,18-20} The spots are elongated in all cases. In addition, streaking in the $[001]$ direction is observed, especially at the lower growth rates. This is consistent with our previous results for growth on exactly (001) substrates at a rate of $0.5 \mu\text{m/h}$ which showed strong $[001]$ streaking.¹⁸ As discussed in the following section, Baxter and co-workers¹⁹ explained the spot elongation as due to inclined [relative to the (001) plane] antiphase boundaries (APBs). The $[001]$ streaking was attributed to the formation of closely spaced (001)-oriented order twin boundaries. These interpretations are generally consistent with the results of Monte Carlo simulations of Ishimaru *et al.*,²¹ also discussed below.

As seen in Fig. 2, a collage of the dark-field electron microscope images obtained for the entire matrix of experiments, the samples grown on exactly (001)-oriented substrates show closely spaced (001) order twin boundaries as well as the inclined APBs. As seen in Fig. 2, for the larger values of ϑ_m , many APBs can be followed from interface to top surface. Others appear to be annihilated some distance into the layer. The domain size in the lateral direction (limited by the APB spacing) for $\vartheta_m = 0^\circ$ increases somewhat as the growth rate is decreased, ranging from approximately 50 Å for growth at $4 \mu\text{m/h}$ to 500 Å at the lowest growth rate of $1 \mu\text{m/h}$, as plotted in Fig. 3. The lateral domain size increases markedly as ϑ_m increases.

The lines separating the domains laterally are confirmed to be APBs from atomic resolution images. Consider, for example, a sample with $\vartheta_m = 3^\circ$ (growth rate = $4 \mu\text{m/h}$). The TEM image, in Fig. 4, clearly shows the 180° change in phase upon crossing the boundary for several APBs. These results confirm the results of Baxter and co-workers¹⁹ and are remarkably similar to the simulated results of Ishimaru *et al.*²¹ The APBs propagate from the substrate toward the surface at a shallow angle of 12° for the samples with $\vartheta_m = 0^\circ$; however, this angle is strongly dependent on the angle of misorientation, measured from the (001) plane. The angle is plotted versus growth rate for the various substrate misorientation angles in Fig. 5. The growth rate has essen-

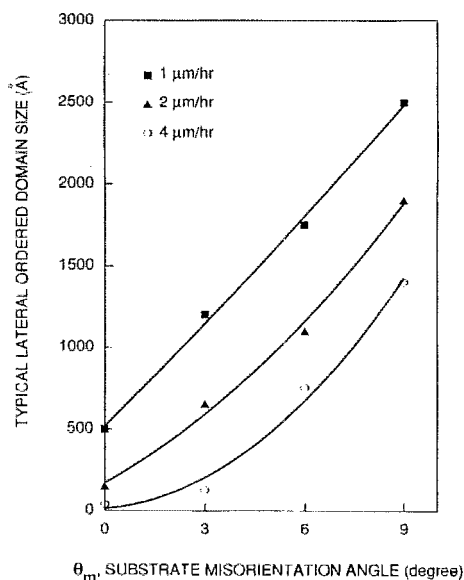


FIG. 3. Lateral domain size (antiphase boundary spacing) vs substrate misorientation for various values of growth rate.

tially no effect while increasing the misorientation angle causes a marked increase in the angle at which the APBs propagate. For $\vartheta_m = 9^\circ$, the direction of propagation is nearly normal to the (001) plane. The data on the effect of substrate misorientation on the direction of propagation of the APBs are consistent with the results of other workers. For example, Bellon *et al.*²⁰ measured an angle of 8° for a growth rate of $0.6 \mu\text{m/h}$ on an exactly (001) GaAs substrate.

As reported previously,^{1-3,20} as the substrate misorientation is increased to 3° , the ordered regions are nearly all the same variant, i.e., one set of superlattice spots essentially disappears, as seen in Fig. 2. In addition, the streaking and distortion of the remaining superlattice spots are markedly reduced. The dark-field images indicate that this is because the distance between the APBs has increased and the (001)

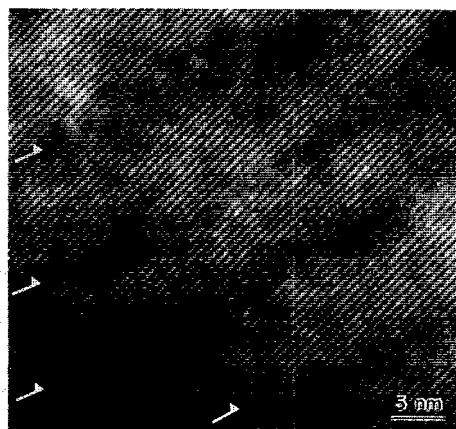


FIG. 4. High-resolution dark-field lattice image of the Cu-Pt ordered structure for GaInP grown at a rate of $4 \mu\text{m/h}$ on a 3° misoriented GaAs substrate. The image was obtained using the $\frac{1}{2}(\bar{1}11)$, $(\bar{1}11)$, and $\frac{3}{2}(\bar{1}11)$ beams. The arrows indicate the antiphase boundaries.

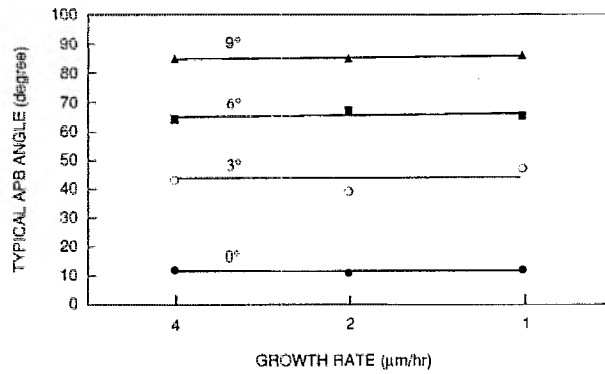


FIG. 5. Angle of antiphase boundaries, measured from the (001) plane, vs growth rate for several values of substrate misorientation.

order twin boundaries have disappeared. The formation of the order twin boundaries was found from the simulations of Ishimaru *et al.*²¹ to be due to the motion of $[\bar{1}10]$ steps across the surface. This type of growth is virtually eliminated when $[\bar{1}10]$ steps are introduced via substrate misorientation in the $[\bar{1}10]$ direction. For misorientations of 6° and 9° the second set of superlattice spots is undetectable and the remaining superlattice spots are nearly perfectly circular.

The degree of order can be judged semiquantitatively from the intensities of the superlattice spots relative to the related zinc-blende lattice spots for the samples with relatively large domains, i.e., for samples with values of ϑ_m of 6° and 9° and for some samples misoriented by 3°. For samples with small domains, relative to the thickness of the TED samples and the size of the selected-area-diffraction aperture, interference effects complicate the interpretation of the electron-diffraction intensity data.²² For the sample with $\vartheta_m=3^\circ$ and a growth rate of 1 $\mu\text{m}/\text{h}$ and for all the samples with larger misorientation angles the TED patterns are obtained from regions containing a single variant of ordered material. Thus, the spot intensity should be a reliable relative measure of the degree of order.²²

The TED patterns in Fig. 1 appear to show a maximum degree of order for samples misoriented by an angle in the neighborhood of 6° for all growth rates with a decrease in the degree of order as the substrate misorientation reaches 9°. An attempt to quantify this data was based on the relative increase in exposure time needed to make the superlattice spots, on the TED negative produced in the TEM, appear the same as the zinc-blende spots obtained with the lower exposure times. The ratio of these two times represents, semiquantitatively, the relative degree of order. These results, plotted in Fig. 6 for growth rates of 1 and 2 $\mu\text{m}/\text{h}$, suggest the maximum order occurs for values of ϑ_m of approximately 5°. This is generally consistent with earlier observations of Kurtz *et al.*⁶ and Buchan *et al.*⁷ who used the band-gap shrinkage, measured using photocurrent and photoluminescence spectroscopy, respectively, to estimate the degree of order. As pointed out by Kurtz *et al.*⁶ the misorientation giving the maximum degree of order is dependent on other growth conditions, primarily the substrate temperature. For a substrate temperature of 670 °C, Buchan *et al.*⁷

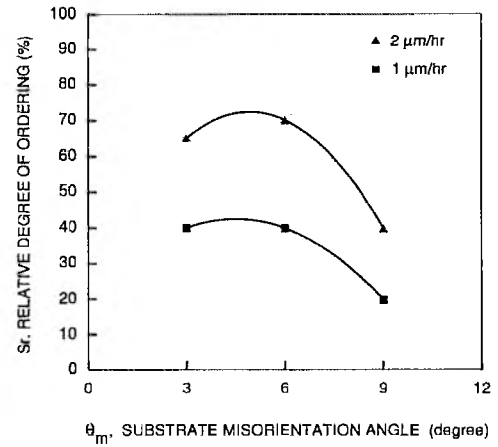


FIG. 6. Relative degree of order, measured from the TED spot intensities as a function of substrate misorientation for several growth rates.

reported a maximum in the degree of order for a misorientation of 6°. For a growth temperature of 675 °C, Kurtz *et al.*⁶ reported the maximum degree of order to occur at a substrate misorientation of approximately 4°. In the current experiments the growth temperature was 670 °C, so the results should be comparable.

The relative difficulty of obtaining high-resolution TEM images for the samples grown with misorientations of 3° suggested that interference effects might still be contributing to weaker superlattice diffraction spots in these samples, especially those grown at 2 and 4 $\mu\text{m}/\text{h}$. This may have resulted in a weakening of the 3° data point for 2 $\mu\text{m}/\text{h}$ in Fig. 6. Thus, we also measured the PL peak position to estimate the degree of order from the relative band-gap energy. The data are listed in Table I. The peak positions, corrected using the data of Kuo *et al.*²³ for deviations of composition from the value giving an exact lattice match, $x=0.516$, are plotted in Fig. 7. For growth rates of 2 and 4 $\mu\text{m}/\text{h}$ the minimum band gap is clearly observed to occur for values of ϑ_m of 4°, in general agreement with the data of Kurtz *et al.*⁶ At a

TABLE I. Substrate misorientation, growth rate, composition, and measured PL peak energy for the samples produced in this study.

ϑ_m (deg)	Growth rate ($\mu\text{m}/\text{h}$)	Composition x (Ga)	Band gap $h\nu$ (meV)
0	4	0.510	1880
3	4	0.516	1856
6	4	0.510	1876
9	4	0.516	1890
0	2	0.516	1881
3	2	0.516	1858
6	2	0.540	1892
9	2	0.516	1908
0	1	0.516	1893
3	1	0.535	1899
6	1	0.516	1916
9	1	0.516	1945

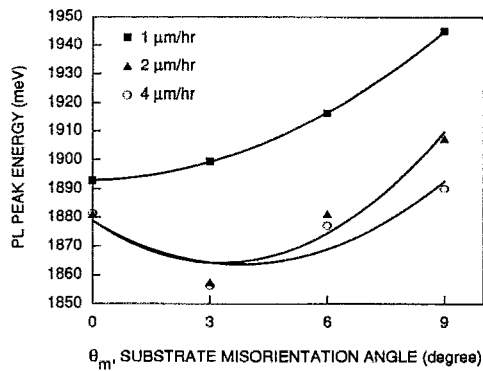


FIG. 7. Peak energy of 10 K photoluminescence peaks, obtained from samples of $\text{Ga}_x\text{In}_{1-x}\text{P}$ grown at several growth rates, vs substrate misorientation. The values of x were approximately 0.516. For samples deviating from this value, the PL energy was corrected using the known dependence of energy band gap on solid composition.

growth rate of $1 \mu\text{m/h}$, the order is lower, presumably due to the effects of annealing during growth.

IV. DISCUSSION

The Cu-Pt ordered structure observed in III/V alloys is formed at the surface during growth.^{1-4,6,20,24} Thus, the kinetic data reported here (excluding the annealing effects, discussed separately) must be related to two factors, the structure of the surface during growth (reconstruction, step structure, step bunching, kink structure, etc.) and the surface diffusion and attachment of species into “half-crystal” sites. The former factors will largely determine the effects of substrate misorientation and both may be major factors in determining the effects of growth rate. Unfortunately, we do not have a detailed understanding of either of these processes, thus, this discussion will necessarily be somewhat qualitative and speculative.

Considering first the substrates with $\vartheta_m = 0^\circ$, our earlier model^{1,2} suggests that the presence of $[110]$ steps, due to thermal roughening or two-dimensional nucleation, moving in both possible directions accounts for the formation of two variants of the Cu-Pt ordered structure. The presence of the high density of (001)-oriented order twin boundaries giving rise to alternate laminae of $(\bar{1}11)$ and $(1\bar{1}1)$ oriented material, as discussed by Baxter and co-workers,¹⁹ gives rise to the pronounced $[001]$ streaking in the TED patterns. The mechanism of formation of this complex structure is unknown, but it is attributed to the motion of $[\bar{1}10]$ steps on the surface.²¹ This may, of course, occur for exactly (001)-oriented growth in the experiments described here.

The origin of the APBs is also suggested by the simulation results of Ishimaru *et al.*²¹ Especially striking is the similarity of the geometry of the predicted APBs to our results for small substrate misorientations, as seen by comparing our Fig. 4 with Fig. 3 of Ref. 21.

The effect of growth rate on the degree of order, seen from the data in Figs. 6 and 7, is generally consistent with the observations of Cao *et al.*²⁵ and Kurtz *et al.*⁶ Cao *et al.* found the PL peak energy to increase with increasing growth

rate in the range from 4 to $12 \mu\text{m/h}$ for a growth temperature of 680°C . The dependence is small near $4 \mu\text{m/h}$. Here we find an increasing PL peak energy as the growth rate decreases from 2 to $1 \mu\text{m/h}$ at 670°C . This is consistent with the data of Kurtz *et al.*,⁶ who reported, for a growth temperature of 675°C , an increasing band-gap energy at both growth rates much lower and much higher than $4 \mu\text{m/h}$. Cao *et al.*²⁵ interpreted their observation of a decrease in the degree of order as the growth rate was increased in terms of the decreased ability of the adatoms to find their lowest energy, i.e., ordered, configuration (on the surface) as the time decreases before an individual layer is covered over by the following layer. Monte Carlo simulations, such as those described in Ref. 21, would be expected to show a decrease in the degree of order as the time for atom exchange on the step edge is reduced. A similar explanation was suggested by Kurtz *et al.*,⁶ considering both the effects of temperature and the step density on the time allowed for Ga/In interchange at a moving surface step. These factors may also partially explain the effect of growth rate on the domain size, with lower growth rates yielding larger domain sizes. At low growth rates the band gap increases due to the “annealing” occurring during the long growth times required for the slow growth rates. The annealing results in the formation of the thermodynamically more stable (in the bulk) disordered structure.

For values of misorientation angle of 3° and larger, the TED patterns indicate that a single variant dominates. This is explained using the model discussed in Refs. 1 and 2 as due to the $[110]$ steps all moving in a common direction. The order twins disappear because growth due to the motion of $[\bar{1}10]$ steps is not significant. The degree of order increases until a maximum is reached at values of $4^\circ \leq \vartheta_m \leq 5^\circ$. At small misorientation angles, one expects an increase in order with increasing ϑ_m simply due to the slower step velocity allowing more atomic interchange at the step to produce the ordered structure. The cause for the decrease in degree of order at high misorientation angles is not known. It may be due to changes in the nature of the surface. Examples would be changes in the step structure, such as step bunching, as discussed below, and/or changes in the surface reconstruction, especially for high values of ϑ_m .¹ Perhaps a more likely explanation would be an increase in the rate of annealing during growth, discussed above, for samples with larger values of substrate misorientation. It has been observed that larger domains anneal more rapidly than smaller domains under otherwise similar conditions.²⁶ Since the domain size increases with increasing misorientation angle (Fig. 3) our results appear qualitatively consistent with this trend.

As the value of ϑ_m increases, the APB spacing becomes much larger (Fig. 3) and the domains become more distinct (Fig. 2). In addition, the angle increases between the (001) plane and the propagating APBs (Fig. 5). Published models are not helpful in understanding this behavior. A problem in our attempt to understand these features of the ordered domains is the lack of even the most elementary specific information about the surface itself during growth. The model of ordering due to step motion described in Refs. 1 and 2 assumes a specific surface reconstruction. The simulations of

Ref. 21 use six adjustable parameters, so they do not require detailed knowledge of the surface.

The kinetic models generally assume that a misoriented substrate is covered by an array of monatomic (really bilayer) steps.¹⁻⁴ This was supported by Suzuki and Gomyo³ who observed the interface in (110) cross sections using TEM images. They found no microfacets, only monolayer steps. However, recent atomic force microscopy studies of GaAs grown by OMVPE indicate that [110]-oriented steps bunch during growth under certain conditions,²⁷ resulting in the formation of facets 7-9 bilayers in height.²⁸ Step bunching was explained by Kasu and Fukui²⁷ in terms of a kinetic mechanism involving the relative probabilities for Ga species being adsorbed at "up" and "down" steps. An alternative, more appealing, explanation is suggested by the results of thermodynamic calculations indicating that the interaction between [110] steps on an (001) surface is attractive.²⁹ The exact structure produced by step bunching is clear from neither experimental evidence nor calculations. Step bunching appears to produce (11̄n) microfacets. A recent article by Friedman *et al.*³⁰ established a general relationship between ordering and the microfacets formed by step bunching on the surface during OMVPE growth.

While no specific model is given here for the effects of substrate misorientation on the direction of propagation and the spacing of the APBs, it is difficult to believe that step bunching would not cause major changes in the growth mode and, in turn, the ordering mechanism.

V. CONCLUSIONS

The growth rate and, particularly, the angle of substrate misorientation have been found to have major influences on the ordered structures observed in Ga_xIn_{1-x}P layers (with $x \approx 0.52$) grown on nominally (001)-oriented GaAs substrates. For example, epilayers grown on substrates with no intentional misorientation at a growth rate of 4 μm/h produce extremely small ordered domains, approximately 50 Å across, separated by antiphase boundaries in the lateral directions. In the [001] (growth) direction the domain size is defined by closely spaced, (001)-oriented order twin boundaries producing alternating variants of the Cu-Pt structure only a few monolayers thick. The APB spacing increases markedly with decreasing growth rate. However, the effect of substrate misorientation is even more dramatic. Misorientation by 3°, 6°, and 9° results in relatively large single domains with no order twins and widely spaced APBs that in many cases propagate from the substrate to the top surface. The APB spacing can be as large as 2500 Å for a misorientation angle of 9° and a growth rate of 1 μm/h. The APBs propagate at an angle that is strongly dependent on the angle of misorientation and nearly independent of growth rate. For $\vartheta_m = 9^\circ$ the APBs propagate at an angle nearly normal to the (001) plane. The degree of order judged from the intensities of superspots, relative to the zinc-blende spots, indicates a maximum degree of order for substrate misorientations of approximately 5° for growth rates of 1 and 2 μm/h. Using the lowering of PL peak energy as a measure of ordering suggests the maximum ordering occurs for substrate misorientations of 4° for growth rates of 2 and 4 μm/h.

ACKNOWLEDGMENTS

This research was supported by the Department of Energy, Basic Energy Sciences Division. The photoluminescence measurements were performed in the J. Dixon Laser Institute and partially supported by the Office of Naval Research.

¹For a general review of this subject, see G. B. Stringfellow and G. S. Chen, *J. Vac. Sci. Technol. B* **9**, 2182 (1991), and G. B. Stringfellow, in *Common Themes and Mechanisms of Epitaxial Growth*, edited by P. Fuoss, J. Tsao, D. W. Kisker, A. Zangwill, and T. Kuech (Materials Research Society, Pittsburgh, PA, 1993), pp. 35-46.

²G. S. Chen and G. B. Stringfellow, *Appl. Phys. Lett.* **59**, 3258 (1991).

³T. Suzuki and A. Gomyo, *J. Cryst. Growth* **111**, 353 (1991).

⁴S. B. Ogale and A. Madhukar, *Appl. Phys. Lett.* **60**, 2095 (1992).

⁵D. S. Cao, A. W. Kimbal, G. S. Chen, K. L. Fry, and G. B. Stringfellow, *J. Appl. Phys.* **66**, 5384 (1989).

⁶S. R. Kurtz, J. M. Olson, D. J. Arent, A. E. Kibbler, and K. A. Bertness, in *Common Themes and Mechanisms of Epitaxial Growth*, edited by P. Fuoss, J. Tsao, D. W. Kisker, A. Zangwill, and T. Kuech (Materials Research Society, Pittsburgh, PA, 1993), pp. 83-88; S. R. Kurtz, J. M. Olson, and A. E. Kibbler, *Appl. Phys. Lett.* **57**, 1922 (1990).

⁷N. Buchan, W. Heuberger, A. Jakubowicz, and P. Roentgen, *Inst. Phys. Conf. Ser.* **120**, 529 (1992).

⁸M. Suzuki, Y. Nishikawa, M. Ishikawa, and Y. Kokubun, *J. Cryst. Growth* **113**, 127 (1991).

⁹T. S. Kuan, T. F. Kuech, W. I. Wang, and E. L. Wilkie, *Phys. Rev. Lett.* **54**, 201 (1985).

¹⁰O. Ueda, Y. Nakata, and T. Fukui, *Appl. Phys. Lett.* **58**, 705 (1991).

¹¹M. Ikeda, E. Morita, A. Toda, T. Yamamoto, and K. Kaneko, *Electron. Lett.* **24**, 1094 (1988).

¹²A. Gomyo, T. Suzuki, S. Ijima, H. Hotta, H. Fujii, S. Kawata, K. Kobayashi, Y. Ueno, and I. Hino, *Jpn. J. Appl. Phys.* **27**, L2370 (1988).

¹³H. R. Jen, M. J. Jou, Y. T. Cherng, and G. B. Stringfellow, *J. Cryst. Growth* **85**, 175 (1987).

¹⁴A. Valster, C. T. H. F. Liedenbaum, N. M. Finke, A. L. G. Severens, M. J. B. Boermans, D. W. W. Vandenhoudt, and C. W. T. Bulle-Lieuwma, *J. Cryst. Growth* **107**, 403 (1991).

¹⁵L. C. Su, S. T. Pu, G. B. Stringfellow, J. Christen, H. Selber, and D. Bimberg, *Appl. Phys. Lett.* **62**, 3496 (1983).

¹⁶S. H. Wei and A. Zunger, *Phys. Rev. B* **39**, 3279 (1989).

¹⁷S. H. Wei and A. Zunger, *Appl. Phys. Lett.* **58**, 2684 (1991).

¹⁸L. C. Su, S. T. Pu, G. B. Stringfellow, J. Christen, H. Selber, and D. Bimberg, *J. Electron. Mater.* **23**, 125 (1994); M. C. Delong, Z. H. Lin, P. C. Taylor, L. C. Su, S. T. Pu, and G. B. Stringfellow, 1993 Electronic Materials Conference, June 1993.

¹⁹C. S. Baxter, W. M. Stobbs, and J. H. Wilkie, *J. Cryst. Growth* **112**, 373 (1991).

²⁰P. Bellon, J. P. Chevalier, E. Augarde, J. P. Andre, and G. P. Martin, *J. Appl. Phys.* **66**, 2388 (1989).

²¹M. Ishimaru, S. Matsumara, N. Kuwano, and K. Oki, *J. Cryst. Growth* **128**, 499 (1993).

²²C. S. Baxter, R. F. Broom, and W. M. Stobbs, *Surf. Sci.* **228**, 102 (1990).

²³C. P. Kuo, S. K. Vong, R. M. Cohen, and G. B. Stringfellow, *J. Appl. Phys.* **57**, 5428 (1985).

²⁴S. Froyen and A. Zunger, *Phys. Rev. Lett.* **66**, 2132 (1991).

²⁵D. S. Cao, E. H. Reihlen, G. S. Chen, A. W. Kimball, and G. B. Stringfellow, *J. Cryst. Growth* **109**, 279 (1991).

²⁶J. E. Williams, H. R. Jen, and K. Meehan, Poloroid Corporation (private communication); P. Gavrilovic, F. P. Dabkowski, K. Meehan, J. W. Williams, W. Stutius, K. C. Hsieh, N. Holonyak, M. A. Shahid, and S. Mahajan, *J. Cryst. Growth* **93**, 426 (1988).

²⁷M. Kasu and T. Fukui, *Jpn. J. Appl. Phys.* **31**, L864 (1992).

²⁸K. Hata, A. Kawazu, T. Okano, T. Ueda, and M. Akiyama, *Appl. Phys. Lett.* **63**, 1625 (1993).

²⁹D. K. Choi, T. Takai, S. Erkoc, T. Halicioglu, and W. A. Tiller, *J. Cryst. Growth* **85**, 9 (1987).

³⁰D. J. Friedman, J. G. Zhu, A. E. Kibbler, J. M. Olson, and J. Moreland, *Appl. Phys. Lett.* **63**, 1774 (1993).